Dalton Transactions

This article can be cited before page numbers have been issued, to do this please use: Y. Jiang, M. Li, X. Liang, J. Mack, M. Wildervanck, T. Nyokong, M. Qin and W. Zhu, *Dalton Trans.*, 2015, DOI: 10.1039/C5DT03256C.

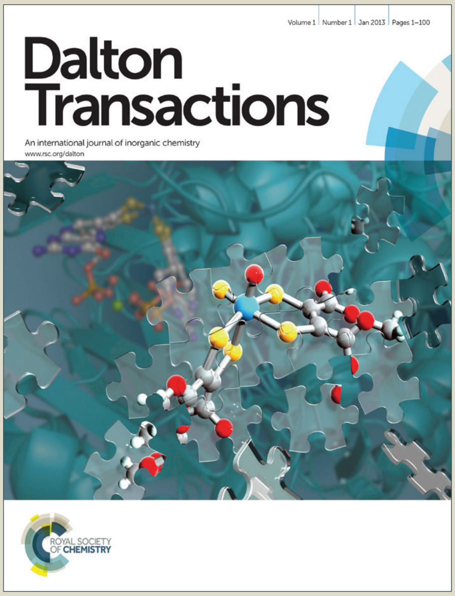

View Article Online
DOI: 10.1039/C5DT03256C

Dalton Transitions

ARTICLE

Lipophilic M(α,α'-OC_5H_{11})$_8$Phthalocyanines (M = H_2 and Ni(II)): Synthesis, Electronic Structure, and their Utility for Highly Efficient Carbonyl Reductions

Received 00th January 20xx,
Accepted 00th January 20xx

DOI: 10.1039/x0xx00000x

www.rsc.org/

Yu Jiang,[a] Minzhi Li,[a] Xu Liang,[a*] John Mack,[b*] Martin Wildervanck,[b] Tebello Nyokong,[b] Mingfeng Qin[a], Weihua Zhu[a*]

A lipophilic and electro-rich phthalocyanine (α,α'-*n*-OC_5H_{11})$_8$-H_2Pc and its nickel(II) complex (α,α'-*n*-OC_5H_{11})$_8$-Ni(II)Pc have been synthesized and characterized. Detailed analysis of the electronic structure were carried out by spectroscopy, electrochemistry, spectroelectrochemistry, and TD-DFT calculations. A series of experiments demonstrate that the (α,α'-*n*-OC_5H_{11})$_8$-Ni(II)Pc complex can be used as catalysts for highly efficient and selective carbonyl reductions.

Introduction

Phthalocyanines (Pcs) have been the subject of considerable research interest over the past few decades in various fields,[1] such as solar cells,[2] molecular electronics and photonics,[3] nonlinear optics,[4] photodynamic therapy (PDT),[5] and also catalysis.[6] The main advantages of phthalocyanine in this regard is that its π-system can absorb and emit strongly in the red/near-infrared (NIR) due to the relatively high molar extinction of the lowest energy π→π* band (usually referred to as the Q band), which is considerably more intense than the corresponding bands in the spectra of porphyrins and tetraazaporphyrins.[7] Also, phthalocyanines are highly thermally stable and have relatively low reactivity due to their heteroaromatic π-systems, and have been reported to have low toxicity.[8] The major drawback faced with most metallo-phthalocyanine (MPc) complexes is that the Q band lies in the 650–680 nm region, while complexes with a band in the near IR region are usually preferred. A red-shift of the Q band reflects a decrease in the HOMO–LUMO gap, and hence is associated with changes in the oxidation and reduction potentials. Although the band can be shifted to longer wavelength through fused-ring-expansion with benzene rings to form naphthalocyanine (Nc)[9] and then anthracocyanine (Ac),[10] the marked destabilization of HOMO level makes these compounds unstable and in the absence of peripheral substituents there are also issues with solubility. On the other hand, the reduction of carbonyl functionalities is one of the most important and basic chemical transformations in organic chemistry. It is an important step in the synthesis of natural products,[11] bulk and fine chemicals.[12]

Numerous methods have been developed to achieve this transformation selectively in the presence of other reducible functionalities[13] using trialkyl boranes with ionic liquid,[14] and metal such as gold[15], manganese[16], iridium[17], platinum[18], ruthenium[19], rhodium[20], osmium[21]. Use of costly metals, stoichiometric amounts of additives and poor selectivity limits their scope. Nickel is abundantly available and found to be effective for carbonyl reduction due to its cost effectiveness over other frequently used transition metals. Although Ni(II)Pcs have been studied as catalysts for carbonyl reduction previously,[22] Ni(II)Pcs with electron rich π-systems are likely to form better catalysts for their reduction. Phthalocyanines with electron-donating substituent groups at the non-peripheral positions have red-shifted Q bands, since there are large MO coefficients at these positions in the HOMO of the π-system and the destabilization of this MO results in a significant narrowing of the HOMO–LUMO gap.[23] Several aryl-substituted carbonyl derivatives are lipophilic thus reactions in high-polar solvent such as methanol or PEG-400 may not be suitable for many of these derivatives. So, Ni(II)Pcs with long alkyl-substituents and deformed structure merit consideration for the carbonyl reductions of lipophilic compounds. *n*-Pentoxy substituents were selected for incorporation at the α,α'-positions, since long alkyl-chains and deformed structures significantly enhance the solubility compared with the regular phthalocyanines.[24]

In this manuscript, the synthesis, characterization, spectroscopy, electrochemistry, spectroelectrochemistry, theoretical calculations of lipophilic M(α,α'-*n*-OC_5H_{11})$_8$-Pcs (M = H_2 and Ni(II)) and its utility for applications on highly efficient carbonyl reductions will be detailed described

---

[a] School of Chemistry and Chemical Engineering, JiangSu University, Zhenjiang 213200, P. R. China. E-mail: sayman@ujs.edu.cn(W. Zhu); liangxuujs@126.com(X. Liang).
[b] Department of Chemistry, Rhodes University, Grahamstown 6140, South Africa. E-mail: j.mack@ru.ac.za

† Electronic Supplementary Information (ESI) available: structural characterization and theoretical calculation data. See DOI: 10.1039/x0xx00000x

View Article Online
DOI: 10.1039/C5DT03256C

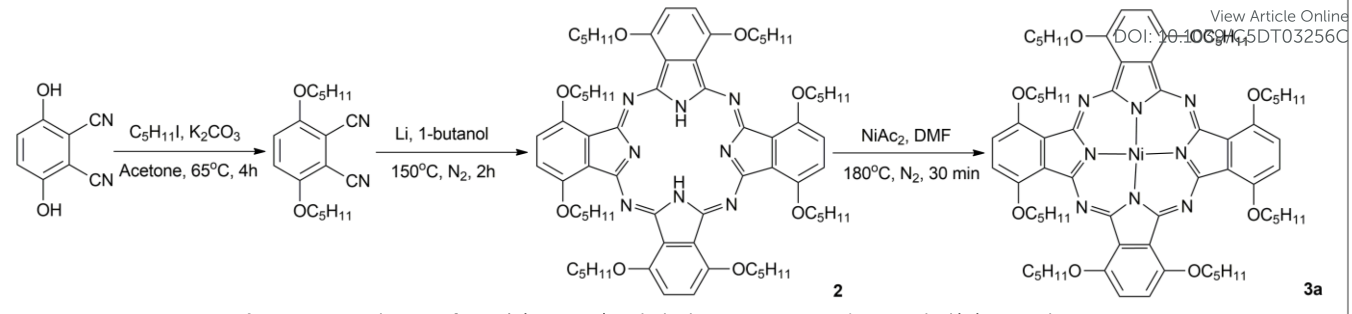

Scheme 1 Synthesis of α, α'-$(C_5H_{11}O)_8$-phthalocyanine **2** and its Nickel(II) complex **3a**.

Experimental

General

^{1}H NMR spectra were recorded on a Bruker AVANCE 500 or Bruker AVANCE 400 spectrometer (operating at 500.13 MHz or 400.03 MHz) using the residual solvent as an internal reference for ^{1}H (δ = 7.26 ppm for $CDCl_3$, δ = 5.32 ppm for CD_2Cl_2). All reagents and solvents were of commercial reagent grade and were used without further purification except where noted. Cyclic voltammetry was performed in a three-electrode cell using Chi-730D electrochemistry station. A glassy carbon disk electrode was utilized as the working electrode while a platinum wire and a saturated calomel electrode (SCE) were employed as the counter and reference electrodes, respectively. An "H" type cell with a fritted glass layer to separate the cathodic and anodic sections of the cell was used for bulk electrolysis. The working and counter electrodes were made from platinum mesh and the reference electrode was an SCE. Both the working and reference electrodes were placed in one compartment while the counter electrode was in other compartment of the cell. UV-visible spectroelectrochemical measurements were performed with a home-made optically transparent thin-layer cell with Pt mesh as the working electrode. The potential was applied using a Chi-730D potentiostat. Time-resolved UV-visible spectra were recorded with a HP 8453A diode array spectrophotometer. All electrochemical and spectroelectro-chemical measurements were carried out under a nitrogen atmosphere. An Agilent HP6890 GC gas chromatography system with a HP5975-MSD detector was used to separate and identify the products of catalytic Carbonyl Reductions. Magnetic circular dichroism (MCD) spectra were recorded on a JASCO J-815 spectrodichrometer equipped with a JASCO electromagnet, which produces magnetic fields of up to 1.6 T (1 T = 1.0 tesla) with both parallel and antiparallel fields. The conventions of Piepho and Schatz are used to describe MCD intensity and the Faraday terms.[25]

Computational methods

The Gaussian 09 software package[26] was used to carry out DFT geometry optimizations for **2** and **3a-c** by using the B3LYP functional with 6-31G(d) basis sets. Ethoxy substituents were used to simplify the calculations. Slightly saddled structures were predicted with N–M–N angles in the central cavity of below 10° for **3a** (3.4 and 3.7°). TD-DFT calculations by using CAM-B3LYP functional, which includes a long-range correction of the exchange potential by incorporating an increasing fraction of Hartree-Fock (HF) exchange as the interelectronic separation increases, was used for **2** and **3a**. This makes it more suitable for studying compounds where there is significant charge transfer in the electronic excited states as is likely to be the case with Pc complexes substituted by bulky *n*-alkoxy substituents at the α, α'-positions.

Synthesis and Characterizations

Synthesis of 1,4-n-OC_5H_{11}-2,3-phthalonitrile. 1,4-$(OH)_2$-2,3-phthalonitrile (1.6 g, 10 mmol) was added to 20 mL of a dry acetone solution containing 1-iodopentane (4.4 g, 22 mmol, 2.2 eq.) and K_2CO_3 (5.5 g, 40 mmol, 4.0 eq). The resulting mixture was gradually heated to 60°C, and the temperature was maintained for 4 h. After removal of the solvent, the reaction mixture was purified by silica gel column chromatography with $CHCl_3$ as the eluent. Recrystallization from $CHCl_3$ and MeOH provided 1,4-*n*-OC_5H_{11}-2,3-phthalonitrile as a white solid compound in 88% yield (2.64 g). ^{1}H NMR (400 MHz, $CDCl_3$): δ = 7.15 (s, 2H; *β*-phenyl), 4.04 (t, *J* = 8.0 Hz, 4H; -OCH_2-), 1.84 (*dd*, J_1=12.0 Hz, J_2 = 8.0 Hz, 4H; -CH_2-), 1.49–1.35 (m, 8H, -CH_2CH_2-), 0.93 (t, *J* = 8.0 Hz, 6H; -CH_3).

Synthesis of H_2-α,α'-n-$(OC_5H_{11})_8$-phthalocyanine (H_2Pc). lithium (56 mg, 8.0 mmol) was added to 6 mL of freshly distilled 1-butanol, and the solution was stirred and heated at 150°C under an N_2 atmosphere until the lithium was completely dissolved. 1,4-OC_5H_{11}-2,3-phthalonitrile (300 mg, 1.0 mmol) was then added and the resulting mixture was gradually heated at 160°C, and the temperature was maintained for 2 h. After removal of the solvent, the reaction mixture was purified by silica gel column chromatography with $CHCl_3$:MeOH (100:3) as the eluent. Recrystallization from $CHCl_3$ and MeOH provided the target compound **2**, as a green solid in 63% yield (2.64 g). MALDI-TOF-MS: m/z = 1203.78 (Calcd. for $C_{72}H_{98}N_8O_8$ $[M+H]^+$ = 1203.70); ^{1}H NMR (500 MHz, CD_2Cl_2): δ = 7.49 (m, 8H; *β*-phenyl), 4.82 (m, 16H; -OCH_2-), 2.19 (m, 16H; -CH_2-), 1.64–1.48 (m, 32H, -CH_2CH_2-), 1.09–0.85 (m, 24H; -CH_3). UV/vis (toluene): λmax [nm] (ε $[M^{-1}\ cm^{-1}]$) = 781 (123000), 735 (61500), 691 (45400), 428 (28400), 324 (34300).

View Article Online
DOI: 10.1039/C5DT03256C

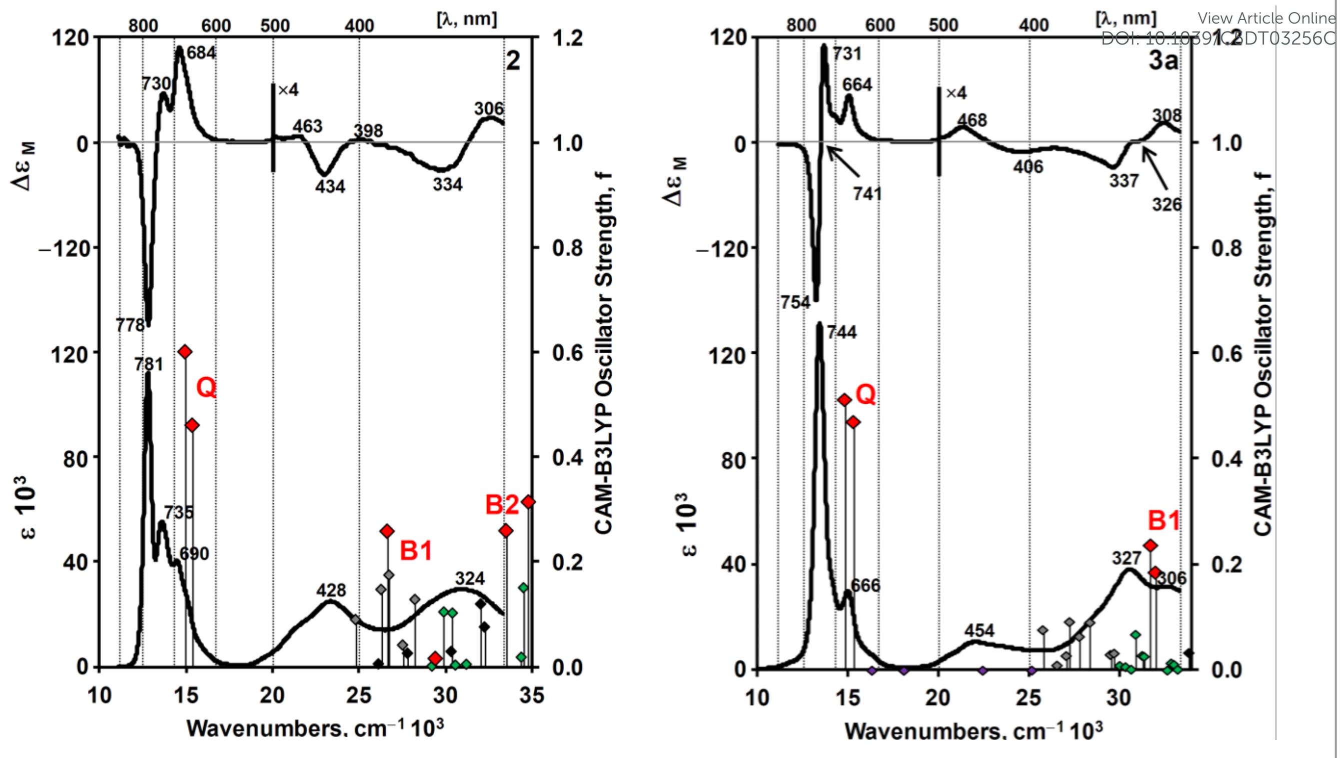

Figure 1 MCD (top) and UV/visible absorption spectra (bottom) of **2** in toluene and **3a** in $CHCl_3$. Calculated TD-DFT spectra are plotted against a secondary axis. The CAM-B3LYP functional was used for the **2** and **3a** calculations with SDD basis sets. Larger red diamonds are used to highlight the Q and B1 bands, while smaller purple, gray, green and black diamonds denote bands associated with transitions involving the 3*d* orbitals, the four frontier π-MOs localized primarily on the peripheral benzo groups, nπ* and the remaining ππ* states, respectively.

Synthesis of Ni(II)-α,α'- $(OC_5H_{11})_8$Pc (Ni(II)Pc). $Ni(CH_3COO)_2{\cdot}4H_2O$ (98 mg, 4.0 mmol, 4.0 eq) and H_2Pc (120 mg, 1.0 mmol) were dissolved in 4 mL of anhydrous DMF, and the solution was stirred and heated at 180°C for 20 min under an N_2 atmosphere. The reaction mixture was poured into ice-water (30 mL) once it had cooled to the room temperature. After filtration, the green solid compound was collected and further purified by silica gel column chromatography with $CHCl_3$:MeOH (100:3) as the eluent. The target compound **3a** was obtained in 88% yield. MALDI-TOF-MS: m/z = 1260.41 (Calcd. for $C_{72}H_{96}N_8NiO_8$ $[M]^+$ = 1260.30); ^{1}H NMR (400 MHz, CD_2Cl_2): δ = 7.49 (br s, 8H; *β*-phenyl), 4.78 (br s, 16H; $-OCH_2-$), 2.20 (m, 16H; $-CH_2-$), 1.63–1.50 (m, 32H, $-CH_2CH_2-$), 1.10~0.98 (m, 24H; $-CH_3$). UV/vis ($CHCl_3$): λ_{max} [nm] (ε [M^{-1} cm^{-1}]) = 744 (133000), 667 (30200), 454 (11500), 327 (39600).

Results and discussions

Synthesis.

H_2Pc **2** was obtained in a good yield (68%) following with the so-called lithium method[1a] by reacting 1,4-OC_5H_{11}-2,3-phthalonitrile in freshly distilled 1-butanol. The ^{1}H NMR signals of **2** in ***Figure S1*** (see *ESI*) are split due to non-planar conformations caused by steric hindrance between the large α,α'-substituents. **2**, is highly soluble in the common organic solvents, such as $CHCl_3$, CH_2Cl_2, ethylacetate, due to the long-alkyl substituents and deformed molecular structure. The Ni(II)Pc **3a** was obtained through metal insertion reactions of the free base phthalocyanine with metal acetate salt and the complexes were isolated by silica gel or alumina column chromatography.

Optical spectra and TD-DFT calculations..

The optical spectra of metal free phthalocyanine **2** were measured in toluene, while those of nickel(II) phthalocyanine **3a** were measured in $CHCl_3$ (**Figure 1**). In its simplest perimeter model description,[27,28] the optical spectroscopy of radially symmetric MPc complexes can be described based on a consideration of perturbations to the molecular orbitals (MOs) arising from the $C_{16}H_{16}^{2-}$ parent hydrocarbon perimeter of the inner ligand perimeter. The MOs of the parent perimeter are arranged in an M_L = 0, ±1, ±2, ±3, ±4, ±5, ±6, ±7, 8 sequence in ascending energy. The highest occupied molecular orbital (HOMO) has an M_L value of ±4 while the lowest occupied molecular orbital (LUMO) has an M_L value of ±5. Michl[28] referred to two frontier π-MOs derived from the HOMO and LUMO of the parent perimeter with nodal planes that lie on the *y*-axis as **a** and **-a**, respectively, while the corresponding MOs which lie on antinodes are referred to as the **s** and **-s** MOs (**Figure 2**). This terminology facilitates the comparison of complexes with differing symmetries. The spin allowed transitions between the **a**, **s**, **-a** and **-s** MOs forms the

View Article Online
DOI: 10.1039/C5DT03256C

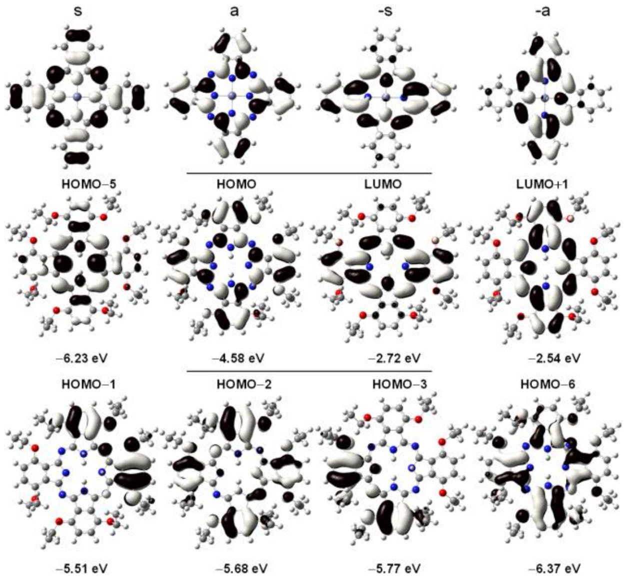

Figure 2 The frontier π-MOs of H_2Pc **2** showing the **a**, **s**, **-a** and **-s** MOs of Michl's perimeter model[21] with M_L = ±4 and ±5 nodal patterns (TOP). The **s** and **-s** MOs have antinodes aligned with the y-axis, while the **a** and **-a** MOs have nodal planes. The nodal patterns of the corresponding MOs are shown (Center) along with those of four occupied frontier π-MOs (Bottom) that are primarily localized on the peripheral benzo groups and are destabilized by the incorporation of electron-donating substituents at the α,α'-positions.

basis of Gouterman's 4-orbital model,[29] which predicts an allowed B transition (ΔM_L = ±1) and a forbidden Q transition (ΔM_L = ±9) arising from the four spin-allowed one-electron HOMO → LUMO transitions. The Stillman group[30] used the simultaneous spectral band deconvolution of the electronic absorption and magnetic circular dichroism (MCD) spectra of phthalocyanines to identify the presence of a second intense absorption band close in the B band region, so the band nomenclature for phthalocyanines was modified to, in ascending energy, the Q (ca. 670 nm), B_1 (ca. 370 nm), B_2 (ca. 330 nm), N (ca. 275 nm), L (ca. 245 nm) and C (ca. 210 nm) bands.[29,30b] The additional information provided by the MCD technique[1a,31] is derived from three highly characteristic spectral features, the Faraday $\mathcal{A}_1$, $\mathcal{B}_0$ and $\mathcal{C}_0$ terms.[31-33] Derivative-shaped Faraday $\mathcal{A}_1$ terms dominate the MCD of most D_{4h} symmetry metal porphyrin and phthalocyanine complexes. These are replaced by coupled pairs of oppositely-signed Gaussian-shaped Faraday $\mathcal{B}_0$ terms, when there is no three-fold or higher axis of symmetry.

As would normally be anticipated for a free-base phthalocyanine,[1a] the Q band of **2** is symmetry-split. The pair of oppositely-signed Faraday $\mathcal{B}_0$ terms in the MCD spectrum at 778 and 730 nm correspond closely to the absorption bands observed at 781 and 735 nm, and there is a shoulder of vibrational intensity at 691 nm. The significant red-shift of the main absorption band can be attributed to the introduction of electron donating substituents at the α, α'-positions,[1a] since it has been demonstrated previously that there is a destabilization of the HOMO of the Pc π-system and hence a narrowing of the HOMO–LUMO gap, due to the presence of large MO coefficients at these positions (**Figures 2** and **3**, and **Table S1** as ESI). In contrast, in the spectra of **3a**, there are $\mathcal{A}_1$ terms or pseudo-$\mathcal{A}_1$ terms at 741, 735 and 825 nm, respectively, correspond to the absorption bands at 744, 738 and 826 nm. The marked differences in the Q band wavelengths of the transition metal complexes of phthalocyanines can be readily explained by the effects of mixing between the doubly degenerate LUMO of the Pc π-system and the 3*d* MOs.[29] The B1 bands of the three metal complexes **3a** can be readily assigned on the basis of the presence of $\mathcal{A}_1$ terms or pseudo- $\mathcal{A}_1$ terms in the MCD spectra at 326, 322 and 349 nm, respectively, slightly to the red of where they are predicted to lie in the TD-DFT calculations (**Figure 1** and **Table 1**). These MCD bands correspond closely to the absorption bands at 327, 322 and 351 nm. The B band of the free-base phthalocyanine **2** is predicted to lie significantly further to the red at 428 nm. In the TD-DFT calculations, a much larger separation is predicted between MOs derived from the HOMO of the $C_{16}H_{16}^{2-}$ parent hydrocarbon perimeter, since there are large MO coefficients on the pyrrole nitrogens of the lower energy **s** MO (**Figures 1** and **2**). In contrast, these atoms lie on nodal planes in the higher energy **a** MOs, so metal complexation has a smaller effect. The bands that lie between the **Q** and $\mathcal{B}_1$ bands in the spectrum of **2**, are probably associated with ππ* states that are destabilized by the incorporation of the alkoxy substituents

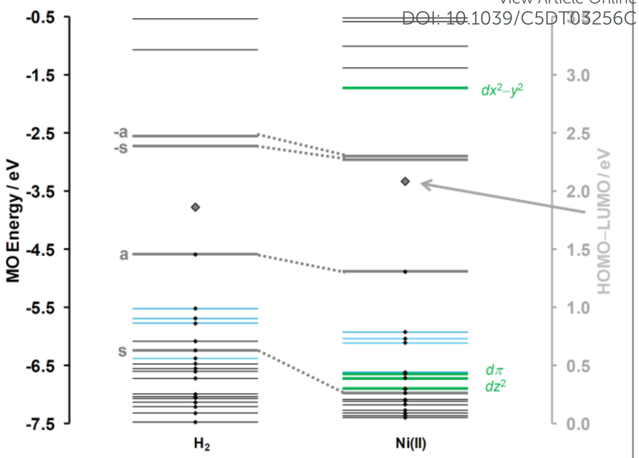

Figure 3 MO energies of **2** (left) and **3a** (right) during B3LYP geometry optimizations with SDD basis sets. Small black diamonds are used to denote occupied MOs. Thicker gray and green lines are used to highlight the four frontier π-MOs associated with Gouterman's 4-orbital model[26] and the 3*d* orbitals of the central metal ion of **3a**, respectively. Blue lines are used to highlight four occupied frontier π-MOs, with MO coefficients largely localized on the four peripheral benzo-moieties, which are destabilized by the presence of the electron-donating alkoxy-substituents. Large dark gray diamonds are used to highlight the HOMO–LUMO gaps and are plotted against a secondary axis.

View Article Online
DOI: 10.1039/C5DT03256C

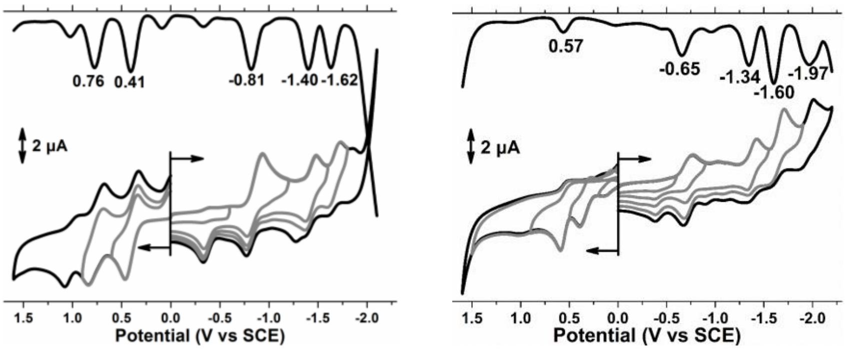

Figure 4 DPV and CV data for **2** in *o*-dichlorobenzene (left) and DMF (right) containing 0.1 M TBAP, scan rate = 100 mV/s.

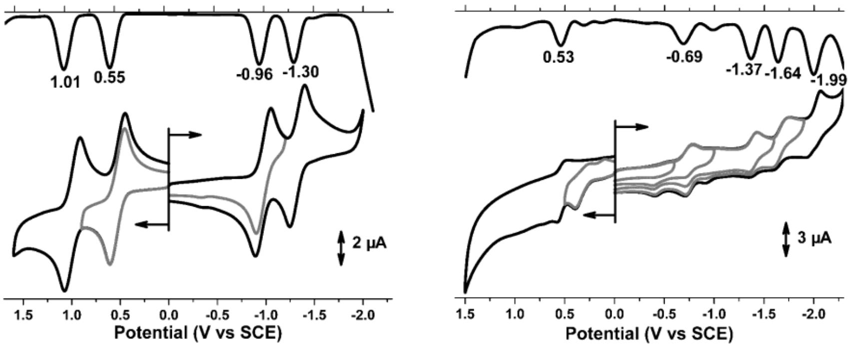

Figure 5 DPV and CV data for **3a** in *o*-dichlorobenzene (left) and DMF (right) containing 0.1 M TBAP, scan rate = 100 mV/s.

(**Figures 2** and **3a**).[34] In TD-DFT calculations, four occupied frontier π-MOs that are localized primarily on the peripheral benzo groups are destabilized relative to the **s** MO that is associated with the B band in the 300–400 nm region. In the spectrum of the metal complex **3a**, the differences of the electronic structures are mainly related to the decrease in the HOMO–LUMO gap, due to the introduction of the electron donating *n*-OC_5H_{11} substituents.

Electrochemistry

When electron-donating substituents are introduced on the phthalocyanine ligand there is an increase in the electron density of the phthalocyanine π-system thereby leading to more difficult ring-reduction and easier ring-oxidation. Additionally, both CV and DPV measurements were also carried out in non-polar *o*-dichlorobenzene, similar electrochemistry curves were observed in the voltammograms, but the $E_{½}$ potential values change significantly due to the large effect of solvent polarity on the electronic structure of the free base phthalocyanine **2**. The cyclic voltammogram (CV) of H_2Pc **2** in non-polar *o*-dichlorobenzene contains two reversible oxidation processes at $E_{½}$ = +0.57 and +0.76 V, and three reversible reduction processes at $E_{½}$ = –1.37, –1.64 and –1.99 V. The gap between the 1st oxidation and reduction potentials ($E^{Ox1} - E^{Red1}$) is ΔE = 2.06 V. When DMF is used to provide a more polar solvation environment, Ni(II)Pc **3a** has an oxidation peak at $E_{½}$ = +0.38 V (**Figure 5**, right), which can be assigned as a ligand oxidation (Pc^{-2}/Pc^{-1}), and the three reduction peaks can be readily assigned to $E_{½}$ = –0.85 V (Pc^{2-}/Pc^{3-}), $E_{½}$ = –1.31 V (Pc^{3-}/Pc^{4-}) and $E_{½}$ = –1.97 V (Pc^{4-}/Pc^{5-}) based on earlier studies of the reduced species of transition metal Pcs,[36] and the predicted energies of the 3*d* orbitals in **Figure 3**. In *o*-dichlorobenzene, Ni(II)Pc **3a** has two reversible oxidation processes at $E_{½}$ = +0.38 and +1.01 V, which can be assigned as a ligand oxidation (Pc^{2-}/Pc^{-}) and (Pc^{-}/Pc^{0}). Two reduction processes were also observed in *o*-dichlorobenzene assigned to $E_{½}$ = –0.85 V (Pc^{2-}/Pc^{3-}), $E_{½}$ = –1.31 V (Pc^{3-}/Pc^{4-}). The significant difference observed in the voltammograms and in the potential values indicate that there is a large solvent effect on the electronic structure of the electron-rich Ni(II)Pc **3a**.

Spectroelectrochemistry

Thin-layer spectroelectochemistry measurements were carried out to develop a better understanding of the redox and optical properties of H_2Pc **2** and Ni(II)Pc **3a**. The measurements were carried out in *o*-dichlorobenzene (**Figure 6**, left side) and DMF (**Figure 6**, right side) to study the impact of solvent polarity. A marked decrease in intensity of the most intense absorption band in the Q band region of H_2Pc **2** is observed in both solvents. Although similar spectral changes are observed in both solvents, they are more pronounced in *o*-dichlorobenzene. A large solvent effect is also observed during the oxidation of **2**. Although loss of the intensity of the Q bands is observed in both solvents, an increase in intensity of a band at 845 nm is only observed in *o*-dichlorobenzene. In contrast in DMF, the main band in the NIR region lies at 778 nm. The optical spectroscopy of the anion radical species of free base phthalocyanine is an area that merits further in depth study.

The ring reduction nature of the first reduction of Ni(II)Pc **3a** was confirmed by thin-layer spectroelectrochemistry. The spectra obtained for the α,α'-alkoxy-substituted Ni(II)Pc **3a** are broadly similar to those reported previously for the unsubstituted nickel phthalocyanine parent complex when the red-shift of the Q and B bands of the neutral complex is taken into consideration.[36a,b,f] Almost identical spectral changes are observed in the Q band region at 744 nm in *o*-dichlorobenzene (**Figure 7**, left side) and DMF (**Figure 7**, right side), but significant differences are observed in the 500–600 nm region and in the emergence of bands in the NIR region at λ = 980 and 860 nm for **3a** in *o*-dichlorobenzene and DMF, respectively. The emergence of bands in this spectral region is usually diagnostic for the formation of [Ni(II)Pc(–3)]$^{–}$ and [Ni(II)Pc(–4)]$^{2–}$ species.[36a,b,f] It is possible that differences in the geometry of the anion radical species, which is known in the absence of a rigid geometry related to axial ligation[37] to be subject to a static Jahn-Teller effect that removes the main four-fold axis of symmetry,[38] could account for this. Markedly different spectra have been reported for [M(II)Pc(–3)]$^{–}$ species on this basis.

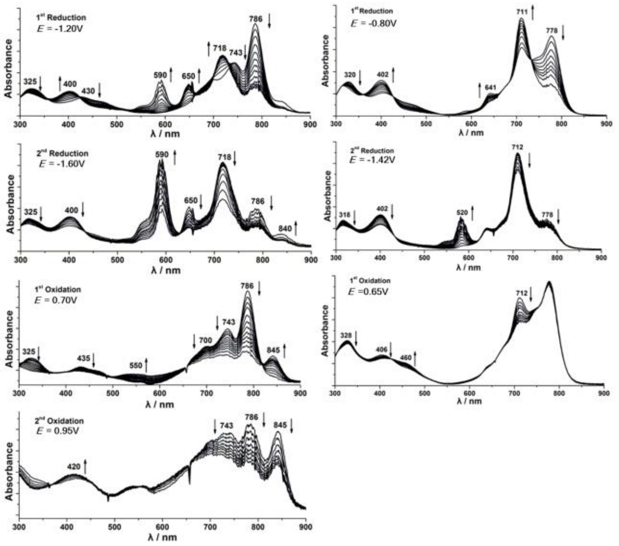

Figure 6 Thin-layer spectroelectrochemistry of **2** in *o*-dichlorobenzene (left side) and DMF (right side) containing 0.1M TBAP.

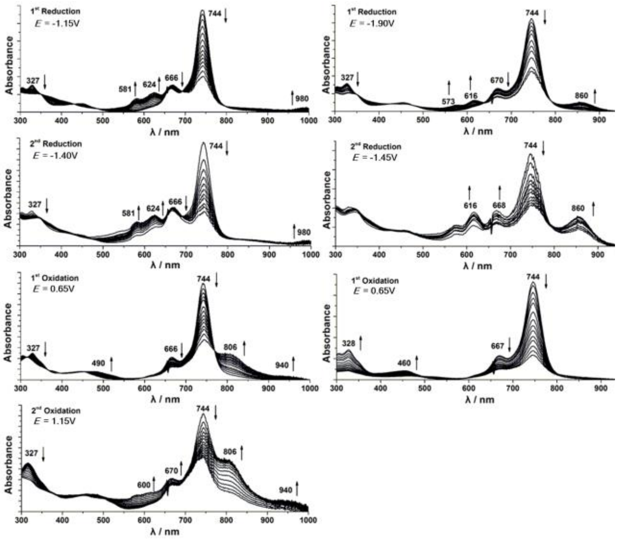

Figure 7 Thin-layer spectroelectrochemistry of **3a** in *o*-dichlorobenzene (left side) and DMF (right side) containing 0.1M TBAP.

Upon oxidation, significant solvent effects are also observed. The diagnostic loss of intensity in the Q band region to form the oxidized [Ni(I)Pc]$^{+}$ species of **3a** is observed in both solvents. Only in the case of the *o*-dichlorobenzene measurements, is there a significant increase in the absorption bands in the near-infrared region at λ = 800 nm and 940 nm. In contrast in DMF, the main band lies at 744 nm. This may be due to a solvent and temperature dependent monomer-dimer equilibrium similar to that reported previously for [Mg(I)Pc]$^{+}$, which was found to have Q bands at 717 nm for the monomeric and dimeric species, respectively, when analyzed in depth using EPR spectroscopy and a simultaneous spectral band deconvolution analysis of the UV-visible absorption and MCD spectra.[39]

Application on Carbonyl Reduction

The use of Ni(II)Pc **3a** for the catalysis of carbonyl reduction reactions has been studied in depth. The use of sodium borohydride ($NaBH_4$) in the absence of any metal under solvent free conditions has been reported.[40] However, the long reaction time and the use of excess $NaBH_4$ limits the scope of this approach.[40a]

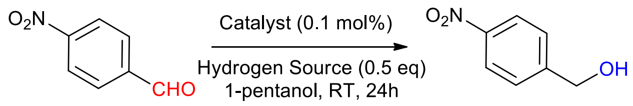

Scheme 2 Optimization of Carbonyl Reduction conditions.

Table 1 Optimized reaction conditions [a].

No.	Catalyst	Hydrogen Source	Yield
1	---	---	n.d.
2	$NiCl_2$	---	n.d.
3	$NiSO_4$	---	n.d.
4	$Ni(CH_3COO)_2$	---	n.d.
5	$NiCl_2$	$NaBH_4$	65%
6	$NiSO_4$	$NaBH_4$	63%
7	$Ni(CH_3COO)_2$	$NaBH_4$	65%
8	---	$NaBH_4$	45%
9	Ni(II)Pc **3a**	$NaBH_4$	>99%
10	Ni(II)Pc **3a**	$NaHCO_3$	n.d.
11	Ni(II)Pc **3a**	NH_2NH_2	n.d.
12	Ni(II)Pc **3a**	H_2O	n.d.
13	Ni(II)Pc **3a**	CH_3COOH	n.d.

Reactions were carried out by using 1.0 mmol of substrate, [catalyst] ratio = 0.1 % mol; yield: GC-yield, Reaction time, 2 h.

Following the synthetic procedure described in **Scheme 2**, 1.0 mmol carbonyl derivatives, 0.1% mol Ni(II)Pc **3** as the catalyst (0.1% eq), and 0.5 mmol sodium borohydride (0.5 eq) were mixed in 2.0 mL 1-pentanol. The reaction solution was stirred at room temperature and the progress of the reaction

View Article Online
DOI: 10.1039/C5DT03256C

was monitored periodically by TLC (silica; petroleum ether/ethylacetate) and GC-MS. Upon completion, the reaction mixture was extracted with diethyl ether (3 mL). The combined diethyl ether fractions were dried under reduced pressure and the crude product was directly characterized by GC-MS. Studies of Ni(II)Pc **3a** catalyzed carbonyl reduction initially focused on the optimization of reaction conditions (**Scheme 2**, **Table 1**). Facile and mild conditions would make **3a** suitable for use in applications. Several catalysts and proton sources were tested to confirm that Ni(II)Pc **3a** reveal highly efficient carbonyl reduction. As expected, only NaBH$_4$ can be used as hydrogen source under current reaction conditions, and the yield of the carbonyl reduction is higher than 99% based on the GC-MS analysis.

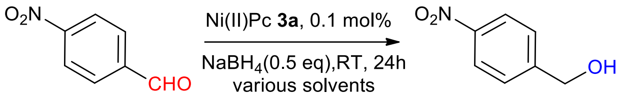

Scheme 3 Optimization of Carbonyl Reduction conditions.

Table 2 Solvent effect of Carbonyl Reduction.

No.	Catalyst	Proton Source	Solvents	Yield
1	Ni(II)Pc **3a**	NaBH$_4$	CHCl$_3$	n.d.
2	Ni(II)Pc **3a**	NaBH$_4$	PhMe	n.d.
3	Ni(II)Pc **3a**	NaBH$_4$	THF	n.d.
4	Ni(II)Pc **3a**	NaBH$_4$	1,4-dioxane	n.d.
5	Ni(II)Pc **3a**	NaBH$_4$	MeOH	65%
6	Ni(II)Pc **3a**	NaBH$_4$	EtOH	63%
7	Ni(II)Pc **3a**	NaBH$_4$	iPrOH	65%
8	Ni(II)Pc **3a**	NaBH$_4$	PEG-400	45%
9	Ni(II)Pc **3a**	NaBH$_4$	1-pentanol	>99%
10	Ni(II)Pc **3a**	NaBH$_4$	1-octanol	95%

Reactions were carried out by using 1.0 mmol of substrate; catalyst ratio = 0.1 % mol; Yield: GC-yield; Reaction time: 20 min.

The effect of solvent polarity on the carbonyl reductions (**Scheme 3**, **Table 2**), was also tested in several kinds of lipophilic solvent including toluene, chloroform, tetrahydrofuran (THF) and 1,4-dioxane. No reaction occurred in lipophilic solvents. Instead, we tried to use methanol, ethanol, PEG-400 and others, and the most satisfactory result was obtained in 1-pentanol and 1-octanol. This is because Ni(II)Pc **3a** contains long *n*-alkyl-chains at the α,α'-positions. The increase in the length of the alkyl-substituents of the alcohol enhances the solubility of **3a**. More usefully, 1-pentanol is much cheaper than PEG-400 and can be recycled by distillation, and it is better than the most satisfied result described previously.

After optimization of the carbonyl reduction conditions was complete, several aryl-aldehydes were tested to confirm the

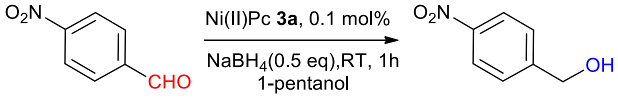

Scheme 4 Optimization of Carbonyl Reduction conditions.

Table 3 Substituent effect of Carbonyl Reduction.

No.	R-aldehyde	Time (min)	Temp. (^{o}C)	Yield[a]	No.	R-aldehyde	Time (min)	Temp. (^{o}C)	Yield[a]
1	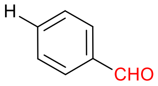	30	25^{o}C	92%	7	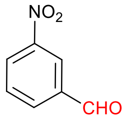	30	25^{o}C	93%
2	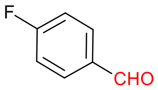	25	25^{o}C	90%	8	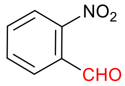	30	25^{o}C	91%
3	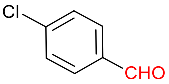	25	25^{o}C	88%	9	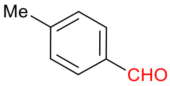	30	25^{o}C	87%
4	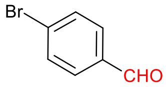	25	25^{o}C	85%	10	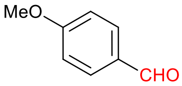	40	25^{o}C	89%
5	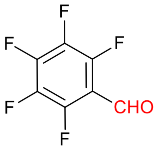	25	25^{o}C	87%	11	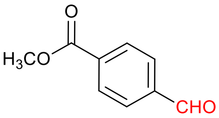	40	25^{o}C	88%
6	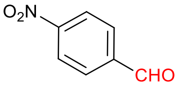	20	25^{o}C	92%	12	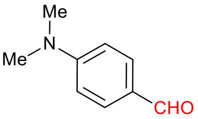	30	25^{o}C	85%

Reactions were carried out by using 1.0 mmol of substrate catalyst ratio = 0.1 % mol; Yield: isolated yield.

substituent effect of the starting materials (**Scheme 4**). Halogen substituted aldehydes with electron-withdrawing abilities were efficiently reduced to the corresponding alcohols in good to excellent yields with no dehalogenation. Methyl, methoxy, dimethylamino, nitrile and acid functionalities remain unaffected during the reduction of the corresponding aldehydes (**Table 3**, entries 4–8). There is no significant change upon changing the electron-donating or withdrawing substituents. The carbonyl reduction results are summarized in the **Table 3**, and the isolated compounds were compared with standard sample by GC-MS analysis.

Conclusions

A lipophilic and electron-rich phthalocyanine (α,α′-*n*-OC$_5$H$_{11}$)$_8$-H$_2$Pc and its nickel(II) complex (α,α′-*n*-OC$_5$H$_{11}$)$_8$-Ni(II)Pc have been synthesized and characterized. The electronic structures have been studied using optical spectroscopy including the UV-visible absorption and MCD techniques, electrochemistry including the use of CV and DPV, spectroelectrochemistry, and TD-DFT calculations. A series of experiments clearly demonstrate that the (α,α′-*n*-OC$_5$H$_{11}$)$_8$-Ni(II)Pc complex can be used as a catalyst to carry out highly efficient carbonyl reductions.

Acknowledgements

Financial support was provided by the NSFC of China (No. 21171076) to WZ and an NRF of South Africa CSUR grant (93627) to JM. The theoretical calculations were carried out at the Centre for High Performance Computing in Cape Town.

Notes and references

1 (a) J. Mack, N. Kobayashi, *Chem. Rev.*, 2011, **111**, 281; (b) C. G. Claessens, U. Hahn, T. Torres, *Chem. Rec.*, 2008, **8**, 75-97.

2 (a) D. Wohrle, D. Meissner, *Adv. Mater.*, 1991, **3**, 129; (b) J. Rostalki, D. Meissner, *Sol. Energy Mater. Sol. Cells,* 2000, **63**, 37; (c) R. Koeppe, N. S. Sariciftci, P. A. Troshin, R. N. Lyubovskaya, *Appl. Phys. Lett.,* 2005, **87**, 244102.

3 (a) P. Turek, P. Petit, J. J. Andre, J. Simon, R. Even, B. Boudjema, G. Guillaud, M. Maitrot, *J. Am. Chem. Soc.* 1987, **109**, 5119; (b) J. Jiang, K. Kasuga, D. P. Arnold, In *Supramolecular Photosensitive and Electroactive Materials* Nalwa, H. S., Ed.; Academic Press: New York, 2001; p 113; (c) D. K. P. Ng, J. Jiang, *Chem. Soc. Rev.*, 1997, **26**, 433; (d) J. Jiang, W. Liu, D. P. Arnold, *J. Porphyrins Phthalocyanines,* 2003, **7**, 459; (e) Y. Chen, W. Su, M. Bai, J. Jiang, X. Li, Y. Liu, L. Wang, S. Wang, *J. Am. Chem. Soc.,* 2005, **127**, 15700.

4 (a) G. de la Torre, P. Vazquez, F. Agullo-Lopez, T. Torres, *Chem. Rev.*, 2004, **104**, 3723; (b) Flom, S. R. In *The Porphyrin Handbook*; Kadish, K. M., Smith, K. M., Guilard, R., Eds.; Academic Press: New York, 2003; Vol. 19, pp 179-190.

5 E. Ben Hur, W. S Chan, In *The Porphyrin Handbook*; Kadish, K. M., Smith, K. M., Guilard, R., Eds.; Academic Press: New York, 2003; Vol. 19, pp 1-35.

6 M. M. Nicholson, In *Phthalocyanine. Properties and Applications*; Lever, A. B. P., Leznoff, C. C., Eds.; VCH: New York, 1993; Vol. 3, pp 71-118.

7 (a) R. P. Linstead, M. J. Whalley, *J. Chem. Soc.* 1952, 4839; (b) S. Shimizu, Y. Haseba, M. Yamazaki, G. Kumazawa, N. Kobayashi, *Chem. Eur. J.,* 2014, **20**, 4822; (c) S. Shimizu, Y. Ito, K. Oniwa, S. Hirokawa, Y. Miura, O. Matsushita, N. Kobayashi, *Chem. Comm.,* 2012, **48**, 3851; (d) J. Mack, L. Sosa-Vargas, S. J. Coles, G. J. Tizzard, I. Chambrier, A. N. Cammidge, M. J. Cook, N. Kobayashi, *Inorg. Chem.,* 2012, **51**, 12820.

8 Y. Rio, M. S. Rodriguez-Morgade, T. Torres, *Org. Biomol. Chem.*, 2008, **6**, 1877-1894.

9 (a) E. F. Bradbrook, R. P. Linstead, *J. Chem. Soc.* 1936, 1739; (b) S. A. Mikhalenko, E. A. Lukuyanets, *J. Gen. Chem. USSR*, 1969, **39**, 2495.

10 W. Freyer, L. Q. Minh, *Monatsh. Chem.,* 1986, **117**, 475-489.

11 M. Kidwai, P. Motshra, R. Mohan, S. Biswas, *Bioorg. Med. Chem. Lett.*, 2005, **15**, 915; (b) M. Kidwai, S. Saxena, R. Mohan, R. Venkataramanan, *J. Chem. Soc. Perkin Trans.*, 2002, **1**, 1845.

12 (a) W. S. Knowles, *Angew. Chem. Int. Ed.,* 2002, **41**, 1998; (b) C, Wang, X. Wu, J. Xiao, *Chem. Asian. J.*, 2008, **3**, 1750.

13 (a) R. Noyori, T. Ohkuma, *Angew. Chem. Int. Ed.*, 2001, **40**, 40; (b) S. Chakraborty, H. Guan, *Dalton Trans.*, 2010, **39**, 7427.

14 G. W. Kabalka, R. R. Malladi, Chem. Commun. 2000, **22**, 2191

15 (a) M. M. Wang, L. He, Y. M. Liu, Y. Cao, H. Y. He, K. N. Fan, *Green Chem.*, 2011, **13**, 602; (b) F. Z. Su, L. He, J. Ni, Y. Cao, H. Y. He, K. N. Fan, *Chem. Commun.*, 2008, **30**, 3531; c) L. He, F. J. Yu, X. B. Lou, Y. Cao, H. Y. He, K. N. Fan, *Chem. Commun.* 2010, **46**, 1553; d) L. He, J. Ni, L. C. Wang, F. J. Yu, Y. Cao Y, H. Y. He, K. N. Fan, *Chem. Eur. J.*, 2009, **15**, 11833.

16 T. Jimenez, E. Barea, J. E. Oltra, J. M. Cuerva, J. Justicia, *J. Org. Chem.*, 2010, **75**, 7022.

17 a) T, Irrgang, D, Friedrich, R, Kempe, *Angew. Chem. Int. Ed.* 2011, **50**, 2183; b) E. L. Roux, R. Malacea, E. Manoury, R. Poli, L. Gonsalvi, M. Peruzzini, *Adv. Synth. Catal.* 2007, **349**, 309; (c) S. M. Lu, C. Bolm, *Angew. Chem. Int. Ed.*, 2008, **47**, 8920; (d) X. Wu, X. Li, A. Z. Gerosa, A. Pettman, J. Liu, A. J. Mills, J. Xiao, *Chem. Eur. J.*, 2008, **14**, 2209.

18 K, Balazsik, K. Szori, G. Szollosi, M. Bartok, *Chem. Commun.*, 2011, **47**, 1551.

19 (a) X. C. Cambeiroa, M. A. Pericas, *Adv. Synth. Catal.*, 2011, 353, 113; (b) K. Everaere, A. Mortreux, J. F. Carpentier, *Adv. Synth. Catal.*, 2003, **345**, 67; (c) A. Z. Gerosa, W. Hems, M. Groarke, F. Hancock, *Platinum Metals Rev.*, 2005, **49**, 158; (d) M. L. Kantam, B. P. C. Rao, B. M. Choudary, B. Sreedhar, *Adv. Synth. Catal.*, 2006, 348, 1970; (e) S. Enthaler, B. Hagemann, S. Bhor, G. A. Kumar, M. K. Tse, B. Bitterlich, K. Junge, G. Erre, M. Beller, *Adv. Synth. Catal.*, 2007, **349**, 853; (f) M. L. Kantam, R. S. Reddy, U. Pal, B. Sreedhar, S. Bhargava, *Adv. Synth. Catal.* 2008, **350**, 2231; (g) J. Ito, S. Ujiie, H. Nishiyama, *Chem Commun.*, 2008, **16**, 1923.

20 (a) Y. Sun, G. Liu, H. Gu, T. Huang, Y. Zhang, H. Li, *Chem Commun.*, 2011, **47**, 2583; b) K. Ahlford, M. J. Ekstrc, A. B. Zaitsev, P. Ryberg, L. Eriksson, H. Adolfsson, *Chem. Eur. J.*, 2009, **15**, 11197; (c) A. N. Ajjou, J. L. Pinet, *J. Mol. Catal. A Chem.*, 2004, **214**, 20.

21 (a) W. Baratta, C. Barbato, S. Magnolia, K. Siega, P. Rigo, *Chem. Eur. J.*, 2010, **16**, 3201; (b) W. Baratta, M. Ballico, A. D. Zotto, K. Siega, S. Magnolia, P. Rigo, *Chem. Eur. J.*, 2008, 14, 2557.

22 V. K. Praveen, S. Upendra, K. Neeraj, B. Manju, K. Vishal Kumar, S. Bikram, *Catal. Lett.*, 2012, **142**, 907.

23 N. Kobayashi, T. Furuyama, K. Satoh, *J. Am. Chem. Soc.*, 2011, **133**, 19642.

24 T. Fukuda, Y. Kikukawa, R. Tsuruya, A. Fuyuhiro, N. Ishikawa, N. Kobayashi, *Inorg. Chem.*, 2011, **50**, 11832.

25 a) S. B. Piepho, P. N. Schatz, In *Group Theory in Spectroscopy with Applications to Magnetic Circular Dichroism*, Wiley: New York, 1983. b) J. Mack, M. J. Stillman, N. Kobayashi, *Coord. Chem. Rev* 2007, **251**, 429.

26 Gaussian 09, Revision D.01, Frisch, M. J.; Trucks, G. W.; Schlegel, H. B.; Scuseria, G. E.; Robb, M. A.; Cheeseman, J. R.;

View Article Online
DOI: 10.1039/C5DT03256C

Scalmani, G.; Barone, V.; Mennucci, B.; Petersson, G. A.; Nakatsuji, H.; Caricato, M.; Li, X.; Hratchian, H. P.; Izmaylov, A. F.; Bloino, J.; Zheng, G.; Sonnenberg, J. L.; Hada, M.; Ehara, M.; Toyota, K.; Fukuda, R.; Hasegawa, J.; Ishida, M.; Nakajima, T.; Honda, Y.; Kitao, O.; Nakai, H.; Vreven, T.; Montgomery, J. A., Jr.; Peralta, J. E.; Ogliaro, F.; Bearpark, M.; Heyd, J. J.; Brothers, E.; Kudin, K. N.; Staroverov, V. N.; Kobayashi, R.; Normand, J.; Raghavachari, K.; Rendell, A.; Burant, J. C.; Iyengar, S. S.; Tomasi, J.; Cossi, M.; Rega, N.; Millam, M. J.; Klene, M.; Knox, J. E.; Cross, J. B.; Bakken, V.; Adamo, C.; Jaramillo, J.; Gomperts, R.; Stratmann, R. E.; Yazyev, O.; Austin, A. J.; Cammi, R.; Pomelli, C.; Ochterski, J. W.; Martin, R. L.; Morokuma, K.; Zakrzewski, V. G.; Voth, G. A.; Salvador, P.; Dannenberg, J. J.; Dapprich, S.; Daniels, A. D.; Farkas, Ö.; Foresman, J. B.; Ortiz, J. V.; Cioslowski, J.; Fox, D. J. Gaussian, Inc., Wallingford CT, 2009.

27 (a) W. Moffitt, *J. Chem. Phys.*, 1954, **22**, 320; (b) W. Moffitt, *J. Chem. Phys.*, 1954, **22**, 1820.

28 (a) J. Michl, *J. Am. Chem. Soc.*, 1978, **100**, 6801. (b) J. Michl, *Pure Appl. Chem.*, **1980**, *52*, 1549. (c) J. Michl, *Tetrahedron* 1984, **40**, 3845.

29 M. Gouterman, In *The Porphyrins*; D. Dolphin, Ed.; Academic Press: New York, 1978; Vol. III, Part A, pp 1-165.

30 (a) T. Nyokong, Z. Gasyna, M. J. Stillman, *Inorg. Chem.*, 1987, **26**, 548-553. (b) T. Nyokong, Z.Gasyna, M. J. Stillman, *Inorg. Chem.*, 1987, **26**, 1087-1095; (c) E. A. Ough, T. Nyokong, K. A. M. Creber, M. J. Stillman, *Inorg. Chem.*, 1988, **27**, 2724; (d) J. Mack, M. J. Stillman, *J. Phys. Chem.*, 1995, **95**, 7935; (e) J. Mack, M. J. Stillman, *Inorg. Chem.*, 1997, **36**, 413.

31 (a) J. Mack, M. J. Stillman, N. Kobayashi, *Coord. Chem Rev.*, 2007, **251**, 429; (b) N. Kobayashi, A. Muranaka, J. Mack, *Circular Dichroism and Magnetic Circular Dichroism Spectroscopy for Organic Chemists*; Royal Society of Chemistry: Cambridge, 2011.

32 S. B. Piepho, P. N. Schatz, *Group Theory in Spectroscopy with Applications to Magnetic Circular Dichroism*; John Wiley and Sons: New York, 1983.

33 P. J. Stephens, *Adv. Chem. Phys.*, 1976, **35**, 197.

34 J. Mack, N. Kobayashi, M. J. Stillman, *J. Inorg. Biochem.*, 2010, **102**, 472-479.

35 N. Kobayashi, S. Nakajima, T. Osa, *Chem. Lett.*, 1992, **21**, 2415.

36 (a) J. Mack, M. J. Stillman, *Inorg. Chem.*, 1997, **36**, 413; (b) P. C. Minor, M. Gouterman, A. B. P. Lever, *Inorg. Chem.*, 1985, **24**, 1894; (c) N. Kobayashi, S. i. Nakajima, H. Ogata, T. Fukuda, *Chem. Eur. J.*, 2004, **10**, 6294. (d) D. W. Clack, J. R. Yandle, *Inorg. Chem.*, 1972, **11**, 1738; (e) C. M. Guzy, J. B. Raynor, L. P. Stodulski, M. C. R. Symons, *J. Chem. Soc. A*, 1969, 997; (f) D. W. Clack, N. S. Hush, J. R. Yandle, *Chem. Phys. Lett.*, 1967, **1**, 157.

37 Y. Kagaya, H. Isago, *Bull. Chem. Soc. Jpn*, 1997, **70**, 2179.

38 (a) J. Mack, M. J. Stillman, *J. Am. Chem. Soc.*, 1994, **116**, 1292; (b) E. W. Y. Wong, C. J. Walsby, T. Storr, D. B. Leznoff, *Inorg. Chem.*, 2010, **49**, 3343.

39 E. Ough, Z. Gasyna, M. J. Stillman, *Inorg. Chem.*, 1991, **30**, 2301.

40 Y. Cao, Z. Dai, B Chen, B. Liu, *J. Chem. Technol. Biotechnol.*, 2005, **80**, 834; (b) B. Cho, S. Kang, M. Kim, S. Ryu, D. An, *Tetrahedron*, 2006, **62**, 8164

View Article Online
DOI: 10.1039/C5DT03256C

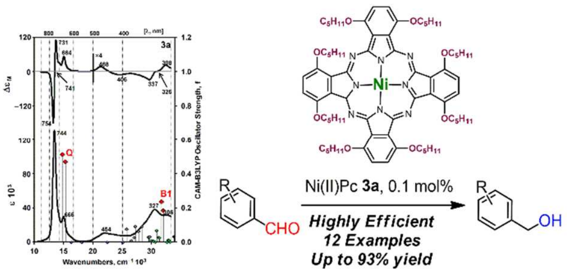

This paper described the electronic structure (α,α'-*n*-OC_5H_{11})$_8$-H_2Pc, (α,α'-*n*-OC_5H_{11})$_8$-Ni(II)Pc and highly efficient carbonyl reductions catalyzed by Ni(II)Pc.